

Polymer Chemistry

Accepted Manuscript



This is an *Accepted Manuscript*, which has been through the Royal Society of Chemistry peer review process and has been accepted for publication.

Accepted Manuscripts are published online shortly after acceptance, before technical editing, formatting and proof reading. Using this free service, authors can make their results available to the community, in citable form, before we publish the edited article. We will replace this *Accepted Manuscript* with the edited and formatted *Advance Article* as soon as it is available.

You can find more information about *Accepted Manuscripts* in the [Information for Authors](#).

Please note that technical editing may introduce minor changes to the text and/or graphics, which may alter content. The journal's standard [Terms & Conditions](#) and the [Ethical guidelines](#) still apply. In no event shall the Royal Society of Chemistry be held responsible for any errors or omissions in this *Accepted Manuscript* or any consequences arising from the use of any information it contains.

ARTICLE

Polystyrene with Hydrophobic End Groups: Synthesis, Kinetics, Interfacial Activity, and Self-assemblies Templated by Breath Figures

Liang-Wei Zhu,^a Bai-Heng Wu,^a Ling-Shu Wan^{a,b,*} and Zhi-Kang Xu^a

Cite this: DOI: 10.1039/x0xx00000x

Received 00th January 2012,
Accepted 00th January 2012

DOI: 10.1039/x0xx00000x

www.rsc.org/

The breath figure method has emerged as a new self-assembly technique to fabricate ordered porous materials which show potential applications in many fields such as size-selective separation membranes. However, it is challenging to customize the structures especially precisely tune the pore size in a wide range. Moreover, the relationship between polymer structure and film morphologies is still unknown. In this paper, we report a facile, effective, and controllable way to manipulate the evolution of morphologies of honeycomb films, which is based on the blends of an amphiphilic block copolymer and polystyrenes with hydrophobic end groups. A series of atom transfer radical polymerization (ATRP) initiators with alkyl or fluorinated groups were synthesized for polystyrenes with hydrophobic end groups. Polymerization kinetics confirmed the viability of these ATRP initiators. Surface segregation behaviors of the hydrophobic end groups were demonstrated by measuring the surface chemical composition and surface free energies. We found that the polystyrenes with hydrophobic end groups form ordered films only at high polymer concentration (40–60 mg/mL); the use of blends of two types of polystyrenes, one of which has a hydrophobic end group whereas the other has a hydrophilic block, can greatly increase the regularity of the honeycomb films and provide the possibility to fine-tune the pore diameter. Moreover, the evolution of surface morphologies of the films can be ideally correlated with the surface free energies of the end-functionalized polymers.

Introduction

Polymer with functional end groups has received increasing attention in the past decades with the development of controlled polymerization techniques, including atom transfer radical polymerization (ATRP),¹ reversible addition–fragmentation chain transfer (RAFT) polymerization,² nitroxide mediated polymerization (NMP),³ ring opening polymerization (ROP),⁴ and anionic polymerization.⁵ Well-defined end groups endow the polymer with advanced or distinctive properties. The functional end groups may enhance the efficiency of solar cells,^{6–8} act as precursors for bioconjugates,^{9,10} introduce stimuli-responsibility,^{11–13} or drive self-assembly.^{14–16} For example, Yu et al. discovered that the aqueous solution of poly(lactic acid-co-glycolic acid)-*block*-poly(ethylene glycol)-*block*-poly(lactic acid-co-glycolic acid), PLGA-*b*-PEG-*b*-PLGA, transfers from a sol state to a reversible sol-gel transition as a function of temperature when end-capped with acetate or propionate group; however, the butyrate end-functionalized polymer forms precipitates.¹⁴ Stöver et al. demonstrated that the hydrophobicity of end groups plays a more important role than molecular weights on the thermo-responsive polymer.¹⁷ Moreover, Kim et al. found that the efficiency of solar cells can be greatly improved by converting the end group of poly(3-hexylthiophene) from bromine to

hydroxyl, ethyl, or perfluoro groups, i.e. from hydrophilic to hydrophobic.⁷

Recently, the breath figure method,^{18,19} which uses water droplets as dynamic templates to form highly ordered honeycomb films, has shown potential applications in fields of photoelectronics,^{20–22} sensors,²³ microcontainers,^{24,25} catalysis,^{26,27} superhydrophobic surfaces,^{28–30} biomaterials,^{31–33} and separation membranes.^{34–36} The structures of honeycomb films, such as pore diameter, pore shape, and multilayered structure, can also be dramatically influenced by the end groups of film-forming polymers. Star polymer, for example, was first utilized to explore the end group effect on the honeycomb structure. Stenzel et al. discovered that the pore diameter decreases from 750 nm to 450 nm when converting the end group of a five-arm star polymer from bromide to pentadecafluoro-1-octanolate.³⁷ Later, Qiao et al. systematically explored the type and number of the end groups of core cross-linked star (CCS) polymers.¹⁶ They found that the pore diameter, regularity, and even the pore shape can be fine-tuned by changing the hydrophilicity of the end groups. Furthermore, they proposed that star polymer with a reversibly photocrosslinkable end group can improve the stability of honeycomb films on non-planar substrates.³⁸

Linear polymers are widely used to fabricate honeycomb structures, owing to the well-defined polymer structure and the simple synthetic process. Highly ordered honeycomb structure

can be easily obtained if a hydrophilic group, such as amino, hydroxyl or carboxyl, is introduced to the polymer chain end.^{19,39-41} Recently, we found that the hierarchical structure, especially the pore diameter, can be significantly and delicately regulated by controlling the hydrophilicity of the end groups.⁴² A multilayered structure with small pore size is obtained if the interaction force between the end group and the water droplet is strong. Similar phenomenon was also reported by Billon and coworkers.⁴⁰ We further revealed that polystyrene with *highly similar* hydrophilic end groups is able to produce *greatly different* honeycomb films.⁴² However, most works are focused on polymers with hydrophilic end groups, and the effects of hydrophobic end groups especially a series of end groups with highly similar structures are still unknown.

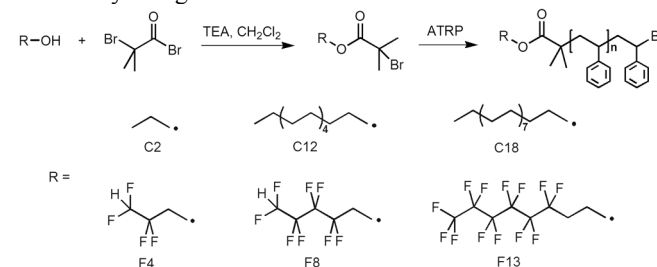
In this work, we aimed to systematically investigate the effects of linear polystyrenes with hydrophobic end groups, from alkyl to fluorinated, on the formation and morphologies of honeycomb films prepared by the breath figure method. First, we synthesized a series of hydrophobic ATRP initiators. Then, these novel initiators were used for the ATRP of styrene, and the polymerization kinetics was investigated. The surface segregation behaviors of the hydrophobic end groups were evaluated by measuring the surface chemical composition and surface free energies. Moreover, honeycomb films were prepared from the resultant homopolymers as well as the blends with an amphiphilic block copolymer. The structures of the honeycomb films were correlated with the surface properties of the polystyrenes with hydrophobic end groups. This work is not only helpful in further understanding of the intrinsic mechanism of breath figure method but also useful in fabricating ordered functional films with adjustable morphologies in a broader range of conditions.

Experimental

Materials

N,N,N',N'-Pentamethyldiethylenetriamine (PMDETA) from Aldrich was distilled with CaH₂ and stored at room temperature in a desiccator. Styrene (St) was obtained from Sinopharm Chemical Reagent Co. and distilled under reduced pressure before use. Copper(I) bromide (CuBr) was stirred in 2% glacial acetic acid aqueous solution overnight, filtered, and washed with absolute acetone under an argon blanket. The compound was dried under reduced pressure at 60 °C overnight. 2-Bromoisobutyryl bromide (BIBB, 98%, Aldrich) was used as received. Ethyl 2-bromoisobutyrate (C2-Br), dodecyl alcohol, 1-hydroxyoctadecane, 2,2,3,3-tetrafluoro-1-propanol, 2,2,3,3,4,4,5,5-octafluoro-1-pentanol, and 3,3,4,4,5,5,6,6,7,7,8,8,8-tridecafluoro-1-octanol were purchased from Energy Chemical without further purification. Triethylamine was refluxed with CaH₂ for 4 h, and dichloromethane was refluxed with P₂O₅ for 2 h prior to use. Deuterated chloroform (CDCl₃, 99.9%) was purchased from Sigma. Methylene iodide (CH₂I₂, 98%) was purchased from Aladdin and used as received. PS-*b*-PDMAEMA ($M_n = 27900$ g mol⁻¹, $M_w/M_n = 1.24$) was synthesized by atom transfer radical polymerization using a reported procedure.⁴³ Poly(ethylene terephthalate) (PET) film was kindly provided by Hangzhou Tape Factory and cleaned with acetone for 2 h before use. The glass substrate was cleaned by piranha solution (2:1 mixture of 98% H₂SO₄ and 30% H₂O₂) for 20 min, rinsed by deionized water, and dried by blowing nitrogen gas before use. Water

used in all experiments was deionized. All other chemicals were analytical grade and used as received.



Scheme 1. Synthetic route for polystyrenes with different hydrophobic end groups.

Synthesis of the Hydrophobic ATRP Initiators

The synthesis route of the initiators is shown in **Scheme 1**. We describe here the synthetic procedure using C12-Br as a typical example. Dichloromethane (30 mL), dodecyl alcohol (2.68×10^{-2} mol, 5 g), and triethylamine (3.23×10^{-2} mol, 3.24 g) were added to a 250 mL three-necked bottle equipped with a constant pressure drop funnel. The bottle was purged with nitrogen for 10 min and cooled in an ice-water bath. Dichloromethane (5 mL) containing BIBB (4.03×10^{-2} mol, 9.25 g) was placed in the constant pressure drop funnel and added dropwise to the reaction bottle. The reaction was kept for 2 h in the ice-water bath followed by 36 h at room temperature. The resulting solution was extracted by saturated aqueous NaHCO₃ solution, drying over anhydrous magnesium sulfate and filtering. Rotary evaporation of the solution results in light yellow liquid, which was further purified by column chromatography using hexane/ethyl acetate (10/1) as the eluent and followed by solvent evaporation under reduced pressure. The resulting colorless liquid was dried in a vacuum oven overnight to achieve the final product C12-Br with a yield of 76.3%.

C12-Br: ¹H NMR (500 MHz, CDCl₃): δ (ppm) 4.17 (2H, CH₂O), 1.93 (6H, 2 × CH₃), 1.68 (2H, CH₂CH₂O), 1.38 (2H, CH₂CH₃), 1.27 (16H, 4 × CH₂CH₂), 0.89 (3H, CH₂CH₃).

C18-Br: ¹H NMR (500 MHz, CDCl₃): δ (ppm) 4.17 (2H, CH₂O), 1.93 (6H, 2 × CH₃), 1.68 (2H, CH₂CH₂O), 1.38 (2H, CH₂CH₃), 1.27 (28H, 7 × CH₂CH₂), 0.89 (3H, CH₂CH₃).

F4-Br: ¹H NMR (500 MHz, CDCl₃): δ (ppm) 5.92 (1H, CHF₂), 4.57 (2H, CH₂O), 1.96 (6H, 2 × CH₃).

F8-Br: ¹H NMR (500 MHz, CDCl₃): δ (ppm) 6.06 (H, CHF₂), 4.67 (2H, CH₂O), 1.96 (6H, 2 × CH₃).

F13-Br: ¹H NMR (500 MHz, CDCl₃): δ (ppm) 4.49 (2H, CH₂O), 2.54 (2H, CH₂CH₂O), 1.94 (6H, 2 × CH₃).

Synthesis of Polystyrenes with Hydrophobic End Groups

The procedure used for synthesizing linear polystyrenes with hydrophobic initiators (e.g., C2-Br) is as follows. ATRP of styrene was performed with a ratio of [St]₀/[C2-Br]₀/[PMDETA]₀/[CuBr]₀ = 200/1/2/1. A 50 mL Schlenk flask was charged with C2-Br (4.363×10^{-4} mol, 42.53 mg), PMDETA (8.726×10^{-4} mol, 181.8 μL), and St (8.726×10^{-2} mol, 10.0 mL) under a nitrogen atmosphere. The solution was degassed by three freeze-pump-thaw cycles. Then, CuBr (4.363×10^{-4} mol, 62.56 mg) was added and another three freeze-pump-thaw cycles were performed. The polymerization was allowed to proceed at a preheated 110 °C oil bath. After that, the flask was quenched in liquid nitrogen to stop the polymerization. Then the reaction mixture was

dissolved with a small amount of tetrahydrofuran (THF), precipitated in methanol, and repeated three times. The obtained product was dried in a vacuum overnight. The details of the obtained polymers are summarized in **Table 1**.

Formation of Honeycomb Films via the Breath Figure Method

The polymers were dissolved in organic solvents with different concentrations. An aliquot of 50 μL for each polymer solution was drop-cast onto a PET substrate placed under a 2 L/min humid airflow (25 $^{\circ}\text{C}$ and $\sim 80\%$ RH). Owing to the condensation of water vapor on the solution surface during the evaporation of organic solvent, the transparent solution turned turbid rapidly. After solidification, the film was dried at room temperature.⁴⁴

Preparation of Dense Films by Drop-Casting

Polymers were dissolved in toluene at a concentration of 20 mg/mL. Dense films were prepared by drop-casting the polymer solutions on glass substrates. Then, the films were annealed at 105 $^{\circ}\text{C}$ in a vacuum condition for 24 h.

Instruments and Measurements

Proton nuclear magnetic resonance (^1H NMR) spectra were recorded on a Bruker (Advance DMX500) NMR instrument

with tetramethylsilane (TMS) as the internal standard and CDCl_3 as the solvent at room temperature.

Molecular weights and molecular weight distribution of the polymers were measured by a PL 220 gel permeation chromatography (GPC) instrument at 25 $^{\circ}\text{C}$, which was equipped with a Waters 510 HPLC pump, three Waters Ultrastaygel columns (500, 103, and 105 \AA), and a Waters 410 DRI detector. THF was used as the eluent at a flow rate of 1.0 mL/min. The calibration of the molecular weights was based on polystyrene standards.

The glass transition temperature (T_g) of the polymers was measured by a differential scanning calorimeter (DSC) on a TA Q200 DSC instrument under nitrogen atmosphere. Polymers with hydrophobic end-groups were sealed in an aluminum sample crucible under nitrogen protection. Then the DSC scan was recorded at a heating rate of 10 $^{\circ}\text{C}/\text{min}$ from 40 to 150 $^{\circ}\text{C}$, followed by immediately cooling from 150 to 40 $^{\circ}\text{C}$ at 10 $^{\circ}\text{C}/\text{min}$, and then again heated from 40 to 150 $^{\circ}\text{C}$ at 10 $^{\circ}\text{C}/\text{min}$. The second heating cycle was recorded for T_g measurement.

A field emission scanning electron microscope (FESEM, Sirion-100, FEI) was used to observe the surface morphology of films after being sputtered with gold using ion sputter JFC-1100. Pore diameter and pore diameter distribution were determined on the basis of the SEM images using Image-Pro Plus software. The boundary value was set at 850 nm to calculate the pore diameter distribution of honeycomb films with bimodal characteristics.

Table 1 Results of Polystyrenes Prepared via Atom Transfer Radical Polymerization

entry	initiator	time (min)	conv. ^c (%)	$M_{n,th}$ ^d	$M_{n,NMR}$ ^e	$M_{n,GPC}$ ^f	PDI ^f
1 ^a	C2-Br	90	37.6	4110	4660	4450	1.07
2 ^a	C2-Br	135	58.4	6270		6520	1.06
3 ^a	C2-Br	150	80.2	8530		8700	1.05
4 ^b	C12-Br	37	17.9	4130	4150	3940	1.06
5 ^b	C12-Br	57	30.8	6800		6580	1.06
6 ^b	C12-Br	77	41.8	9100		8780	1.06
7 ^b	C18-Br	35	17.6	4160	3890	4000	1.08
8 ^b	C18-Br	53	28.6	6450		6280	1.06
9 ^b	C18-Br	80	43.9	9630		9230	1.06
10 ^b	F4-Br	46	17.6	3940	4420	4340	1.06
11 ^b	F4-Br	58	27.9	6090		6560	1.06
12 ^b	F4-Br	84	40.1	8620		9370	1.06
13 ^a	F8-Br	77	34.8	4000	4130	4170	1.06
14 ^a	F8-Br	190	55.0	6100		6450	1.05
15 ^a	F8-Br	280	79.1	8600		9100	1.05
16 ^b	F13-Br	34	16.9	4030	4300	4230	1.07
17 ^b	F13-Br	50	26.7	6070		6380	1.06
18 ^b	F13-Br	90	39.1	8650		9180	1.05

^aReaction conditions: $[\text{St}]_0/[\text{I}]_0/[\text{PMEDTA}]_0/[\text{CuBr}]_0 = 100/1/2/1$, polymerization at 110 $^{\circ}\text{C}$. ^bReaction conditions: $[\text{St}]_0/[\text{I}]_0/[\text{PMEDTA}]_0/[\text{CuBr}]_0 = 200/1/2/1$, polymerization at 110 $^{\circ}\text{C}$. ^cCalculated by the gravimetric method. Conv. (%) = W_p/W_{St} , where W_p and W_{St} are weights of the resultant polymer and styrene in feed, respectively. ^dTheoretical number-average molecular weight, $M_{n,th}$, was calculated according to $M_{n,th} = [\text{St}] \times M_{St} \times \text{conv.}/[\text{I}] + M_I$. ^e $M_{n,NMR}$ determined by ^1H NMR (500 MHz) in CDCl_3 . ^fGPC using differential refractive index detection vs. linear polystyrene standards.

Static contact angles were measured on the dense films by a Drop-Meter A-200 contact angle system (MAIST Vision Inspection& Measurement Ltd. Co.) at room temperature using deionized water and CH₂I₂ as working liquids. The average values calculated from at least five parallel measurements are reported. The surface free energies of the samples were calculated from the static contact angles θ using Owens method:

$$(1 + \cos\theta)\gamma_l = 2(\gamma_s^d \gamma_s^p)^{1/2} + 2(\gamma_l^d \gamma_l^p)^{1/2}$$

$$\gamma_s = \gamma_s^d + \gamma_s^p$$

where γ_l and γ_s are the surface free energies of the liquids and solid surfaces, respectively. Superscripts *d* and *p* denote the dispersion and polar component, respectively. The dispersion and the polar force components of the surface free energy of water are 21.8 and 51.0 mJ/m², respectively, and those of CH₂I₂ are 48.5 and 2.3 mJ/m².⁴⁵

X-ray photoelectron spectroscopy (XPS) analyses were performed on a RBD upgraded PHI-5000C ESCA system (Perkin Elmer, USA) with Al K α radiation ($h\nu = 1486.6$ eV). In general, the X-ray anode was run at 250 W and the high voltage was kept at 14.0 kV with a detection angle at 54°. The base pressure of the analyzer chamber was about 5×10^{-8} Pa. To compensate for surface charging effect, all survey spectra were referenced to the C_{1s} hydrocarbon peak at 284.6 eV.

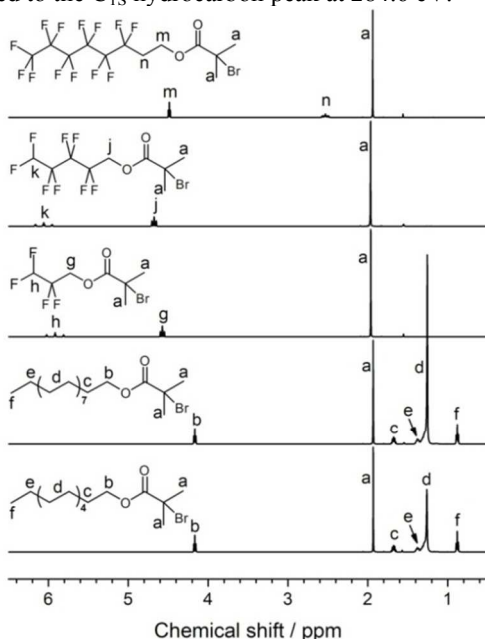


Fig. 1 ¹H NMR spectra of C12-Br, C18-Br, F4-Br, F8-Br and F13-Br (from bottom to top).

Results and discussion

Synthesis and Characterization of Chain-End-Functionalized Polystyrenes

Six hydrophobic initiators containing alkyl chains or fluorine atoms were synthesized by reacting R-OH with 2-bromoisobutryl bromide, and then used to initiate ATRP of styrene under bulk condition at 110 °C (Scheme 1). Fig. 1 shows ¹H NMR spectra of the initiators. The characteristic peaks in the spectra can be well assigned to the protons in these initiators, which are summarized in the experimental section. Table 1 lists the results of polystyrenes with different

molecular weights. The polymers have narrow molecular weight distribution (PDI ≤ 1.08). And, the experimental GPC molecular weights are close to the theoretical values calculated from the monomer conversions. It can be concluded that the polymerization is well controlled. Fig. 2 is the ¹H NMR spectrum of a typical polymer. The terminal methyne proton (-CHBr) at the chain end is located at 4.6–4.4 ppm and the aromatic protons of polystyrene are between 7.2–6.2 ppm. The integral ratio of these two peaks provides an additional mean of calculating the molecular weights ($M_{n,NMR}$). Here we chose the terminal methyne proton (-CHBr) other than protons in the initiator part to calculate the molecular weights of the polymers. It is because that, on the one hand, the protons in the alkyl initiators overlap with the backbone of polystyrene; on the other hand, the integral ratio of the proton in fluorinated initiators (-CHF₂) to the terminal methyne proton (-CHBr) is very close to 1 (e.g., $\sim 1.00/1.07$ for F8-PS). As noted in Table 1, the values of $M_{n,NMR}$ are in good consistent with those of $M_{n,th}$ and $M_{n,GPC}$. The GPC traces (Fig. S1, Supplementary Information, SI) of the obtained polystyrenes are unimodal and symmetrical, which further reveals the viability of these hydrophobic ATRP initiators.

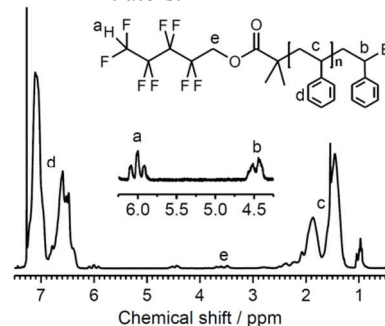


Fig. 2 ¹H NMR spectrum of F8-PS.

We further evaluated the hydrophobic ATRP initiators by studying the polymerization kinetics. Fig. 3 displays the first-order kinetic plots for the bulk polymerization of styrene with the hydrophobic initiators. The monomer consumption increases linearly with time, suggesting that the radical concentration is constant, the termination is negligible, and side reactions can be effectively avoided in the polymerization. In addition, each sample exhibits a narrow molecular weight distribution (PDI ≤ 1.08). Assisted proofs include the consistent values of $M_{n,NMR}$, $M_{n,th}$, and $M_{n,GPC}$ (Table 1) and the unimodal GPC curves (Fig. S1, SI). As a result, we conclude that the polymerization initiated with the hydrophobic initiators proceeds in a controlled manner. Specifically, the apparent rate constants (k_p^{app}) of the polymerizations are less affected by the hydrophobic groups of the initiators.

It is generally accepted that the glass transition temperature (T_g) of a polymer can be affected by its end groups.^{46,47} DSC curves of the polymers with a molecular weight of ~ 9000 g/mol are shown in Fig. 4. It can be seen that the T_g values of alkyl-end-functionalized polystyrenes gradually decrease with the length of alkyl chain (C2-PS > C12-PS > C18-PS), while no obvious changes for polystyrenes initiated with the fluorinated initiators. The reduction of T_g can be described as a result of increased flexibility to polystyrene provided by the long alkyl end group, which has good compatibility with the main chain of the polymer.⁴⁸ However, the fluorinated end group is incompatible with polystyrene,⁴⁹ showing less influence on the values of T_g .

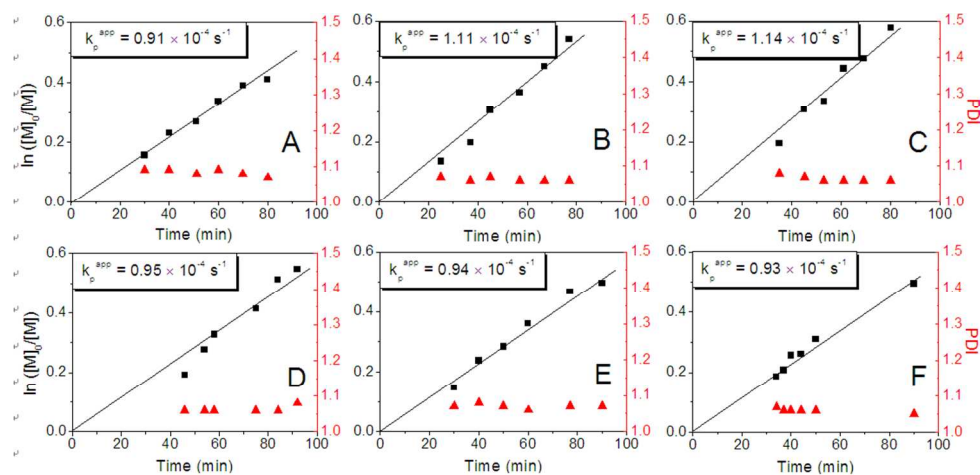


Fig. 3 First-order kinetic plots for the bulk polymerization of St initiated by (A) C2-PS, (B) C12-PS, (C) C18-PS, (D) F4-PS, (E) F8-PS, and (F) F13-PS. Polymerization conditions: $[St]_0/[I]_0/[PMEDTA]_0/[CuBr]_0 = 200/1/1/2$, $110 \text{ }^\circ\text{C}$.

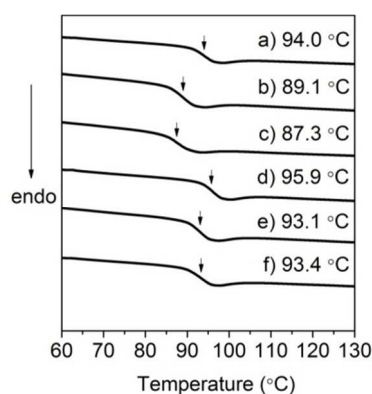


Fig. 4 DSC curves of (a) C2-PS, (b) C12-PS, (c) C18-PS, (d) F4-PS, (e) F8-PS, and (f) F13-PS.

Interfacial Activity of the Chain-End-Functionalized Polystyrenes

The end group of a polymer has great influences on the surface properties, such as wettability, chemical resistance, adhesion, and biocompatibility.⁴⁹⁻⁵³ Here, we compared the surface properties, including surface free energies and surface chemical compositions, of dense films prepared from the homopolymers ($M_n \approx 9000 \text{ g/mol}$) with hydrophobic end groups (Table 2). The dense smooth films were prepared via a drop-casting method and followed by annealing at $105 \text{ }^\circ\text{C}$ for 24 h to drive the low

surface energy components, fluorinated groups or alkyl groups, segregate to the film surface to satisfy the thermodynamic requirements for a minimal surface free energy.⁵⁴ It can be seen that the water and oil contact angles gradually increase with increasing alkyl chain length and the number of fluorine atoms; accordingly, the free surface energies exhibit a reverse trend. In addition, it is reasonable that polystyrenes with fluorinated end groups possess lower surface free energies than those with alkyl end groups.

XPS was further utilized to examine the surface chemical composition. It can be seen that the peak intensity of fluorine element increases obviously (Fig. S2, SI). Considering that XPS is a high-sensitive technique for surface characterization, the calculated ratios of fluorine to carbon elements (F/C) reflect the chemical composition at the film surface within a depth of several nanometers (Table 2). On the other hand, the theoretical bulk composition can be estimated on the basis of the molecular weights, which are listed inside the parentheses in Table 2. The results strongly confirm that the fluorinated groups are able to migrate to the film surface, leading to higher fluorine content at the film surface than in the bulk. Furthermore, it should be noted that polystyrene end-capped with long fluorine groups (F13-PS) are more effective to segregate at the film surface with a much higher F/C ratio at film surface.

Table 2 Contact Angles, Surface Free Energies, and Surface Chemical Composition of Dense Films Prepared from PS ($M_n \approx 9000$) with Hydrophobic End Groups

Polymer	$\theta(\text{H}_2\text{O})/^\circ$	$\theta(\text{CH}_2\text{I}_2)/^\circ$	$\gamma_s^d/\text{mJ m}^{-2}$	$\gamma_s^p/\text{mJ m}^{-2}$	$\gamma_s/\text{mJ m}^{-2}$	F/C ^a
C2-PS	91.8±1.1	20.0±1.6	48.16	0.16	48.32	
C12-PS	96.0±0.2	22.1±1.6	48.25	0.01	48.26	
C18-PS	94.5±0.8	26.3±0.8	46.27	0.06	46.33	
F4-PS	96.9±0.8	30.8±1.7	44.76	0.01	44.77	0.51(0.56)
F8-PS	98.7±1.0	33.4±1.4	43.81	0.01	43.82	1.52(1.18)
F13-PS	100.2±0.5	37.4±1.1	41.99	0.25	42.24	4.97(1.92)

^a Ratios of F to C elements calculated from XPS($M_{n,\text{GPC}}$).

Formation of Honeycomb-Patterned Porous Films from the Homopolymers with Hydrophobic End Groups

Ordered honeycomb films can be prepared in a simple bottom up process via the breath figure technique. The regularity of the films is influenced by various factors, including polymer structure, molecular weight, concentration, solvent, and humidity.^{55,56} To elucidate the effects of hydrophobic end groups on the film structure, three groups of polystyrenes with relatively low molecular weight ($M_n \approx 4000$, 6500, and 9000 g/mol) were synthesized to maximize the effects of chain end groups. In view of the difficulty in fabricating ordered honeycomb films from linear polystyrene without any hydrophilic end groups or blocks, we first investigated the effects of solvents, molecular weights, and polymer concentrations to obtain optimal conditions for film formation.

Effect of solvents on the surface morphology of the honeycomb films are shown in **Fig. S3** (SI). All of the used solvents are good solvents for polystyrene. It can be seen that dichloromethane with the highest vapor pressure (58.2 kPa at 25 °C) gives films with the smallest pore size, mainly owing to the shortened growing time of condensed water droplets. No surface pores can be obtained when a low vapor pressure solvent was used, e.g., toluene (3.79 kPa at 25 °C). Chloroform and tetrahydrofuran do not lead to ordered structure. In relative

terms, the polymer forms ordered honeycomb films in CS_2 although some defects can still be observed.

Polystyrenes with different molecular weights were used to fabricate honeycomb films in CS_2 at a concentration of 10 mg/mL (**Fig. S4**, SI). Overall, the films are not very ordered; relatively ordered structures are obtained from polystyrenes with higher molecular weights. That means polystyrenes with hydrophobic end groups are not able to effectively stabilize condensed water droplets at this concentration. Coalescence of the condensed water droplets can be clearly found, for example, for the film prepared from C2-PS with a M_n of 4000 g/mol. Evidently, polymer with higher molecular weight has higher solution viscosity,⁵⁷ which is conducive to stabilize the condensed water droplets from coalescing. On the other hand, the evaporation rate of solvent decreases with molecular weight due to lower vapor pressure induced by higher molecular weight.⁵⁸ Rapid evaporation of solvent results in fast condensation of water droplets onto the solution surface. Therefore, the comprehensive factors make it difficult to avoid the coalescence behavior in the system of low-molecular-weight polystyrenes with hydrophobic end groups. Taking into account the above-mentioned results and the fact that the end group effect may be ignored for polymers with too high molecular weights, polystyrenes with a M_n of ~ 9000 g/mol are used for further study.

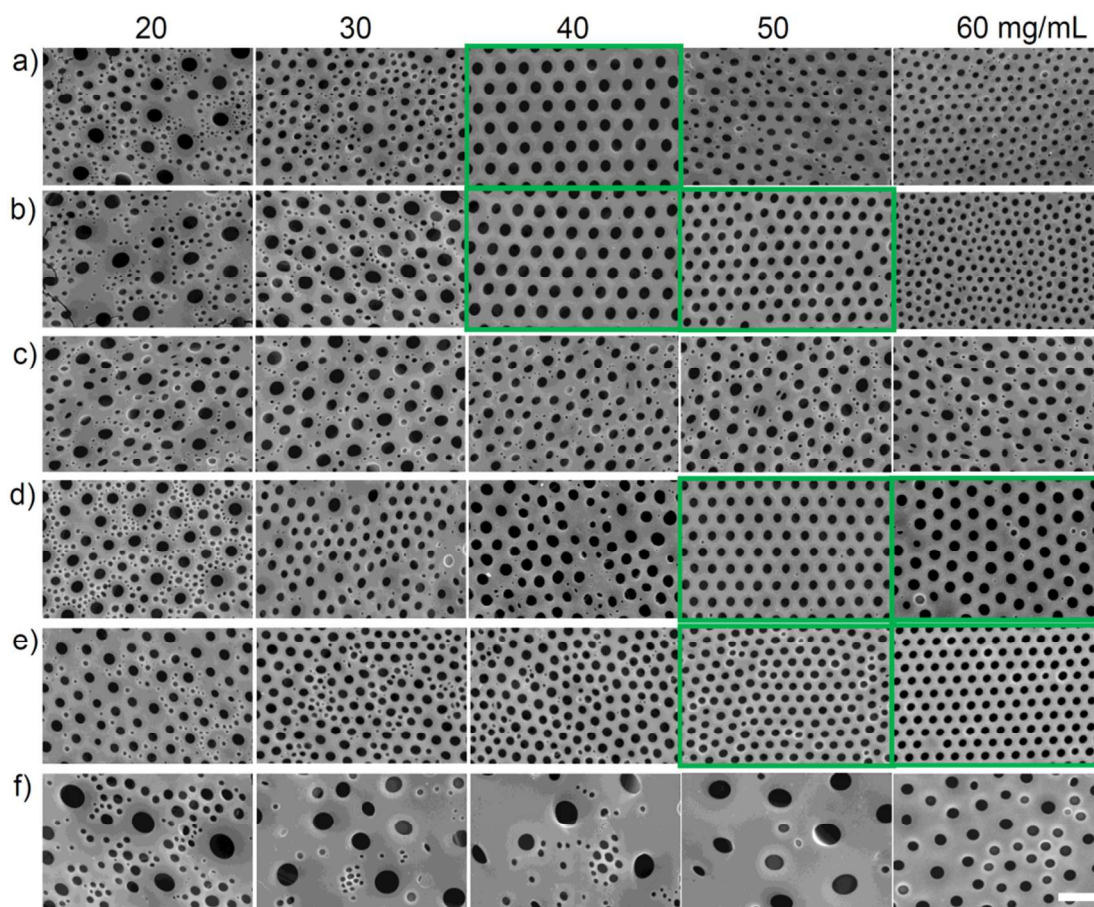


Fig. 5 SEM images of honeycomb films prepared from PS with hydrophobic end groups at different concentrations ranging from 20 to 60 mg/mL. (a) C2-PS, (b) C12-PS, (c) C18-PS, (d) F4-PS, (e) F8-PS, and (f) F13-PS. The scale bar is 5 μ m.

Polymer concentration is an important influencing factor. **Fig. 5** displays SEM images of honeycomb films prepared at different polymer concentrations. It can be seen that ordered honeycomb films form only at relatively very high polymer

concentration (40–60 mg/mL, images marked with green border). Irregular structures appear when the concentration is too low or too high. These results are reasonable and can be explained as follows. If the concentration is too low, it is impossible to stabilize the water droplets from coalescing by depositing at the interface of water droplets and the polymer solution, causing irregular structures. On the contrary, too high concentration means high solution viscosity, which prevents the water droplets from sinking into the solution and weakens Marangoni convection, leading to poor arrangement of water droplets. Similarly, even for an amphiphilic block copolymer such as PS-*b*-PDMAEMA that has been demonstrated in our previous work to be a very good film-forming material at low concentration such as 2 mg/mL,⁵⁹ it cannot form ordered honeycomb film at 10 mg/mL (Fig. S5, S1). Fig. 6 summarizes the effects of concentration, where green circle means well-ordered films while red triangle means disordered. Interestingly, polystyrenes with shorter alkyl chain and fewer fluorine atoms are more likely to form ordered structure at relatively low concentration. Moreover, it can be seen that C18-PS and F13-PS cannot form ordered films even increasing the concentration to 60 mg/mL. Overall, polystyrenes with

hydrophobic end groups are less capable of interfacial stabilization, and hence higher concentration is needed.

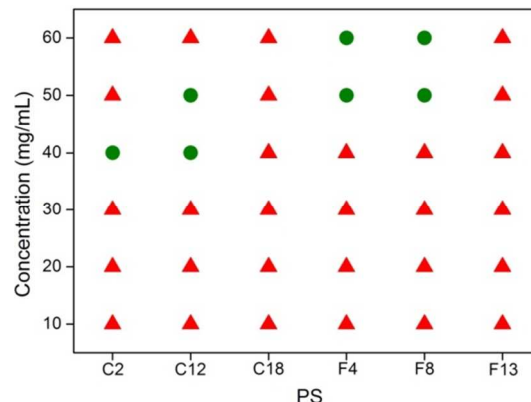


Fig. 6 Diagram of the regularity of honeycomb films prepared from PS with hydrophobic end groups at different concentrations. Green circle means well-ordered films while red triangle means disordered films.

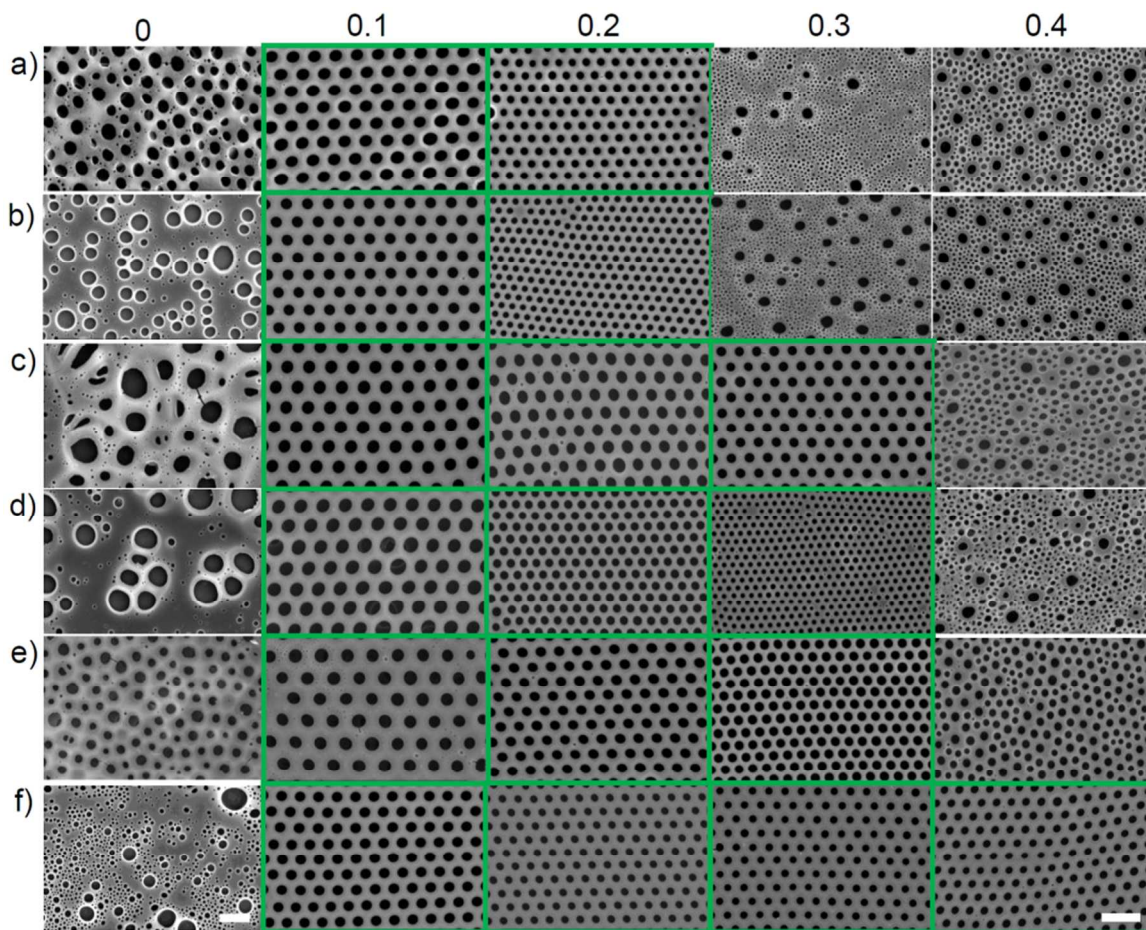


Fig. 7 SEM images of honeycomb films prepared from the mixture of PS and PS-*b*-PDMAEMA at a total concentration of 10 mg/mL. From left to right the weight fraction of PS-*b*-PDMAEMA in the blends changes from 0 to 0.4. (a) C2-PS, (b) C12-PS, (c) C18-PS, (d) F4-PS, (e) F8-PS, and (f) F13-PS. The scale bar is 20 μm for the first column and 5 μm for all the other samples.

Formation of Honeycomb-Patterned Porous Films from the Blends of an Amphiphilic Block Copolymer and the Polystyrenes with Hydrophobic End Groups

As mentioned above, ordered honeycomb films can be obtained from the hydrophobic polymers only at high concentration. However, it is well known that it is much easier to fabricate highly ordered honeycomb films from polymers with polar end groups or blocks by the dynamic breath figure method, and the optimal concentration is generally lower than 10 mg/mL. Blending the polystyrenes with an amphiphilic block copolymer is speculated to remarkably lower the concentration, saving polymer consumption; more importantly, it may provide an avenue to tune the morphologies of the self-assembled films over a wide range.

Fig. 7 shows the SEM images of honeycomb films prepared from the blends of polystyrenes and PS-*b*-PDMAEMA (BCP) in CS₂ at 10 mg/mL. The weight fraction of BCP in the mixture varies between 0 and 0.4. The morphology of the films evolves with the content of BCP. Pure polystyrene with hydrophobic end groups (homopolymer) only forms irregular structures. After adding a certain amount of amphiphilic BCP, highly ordered films are obtained. Significantly, just by blending 10 wt.% BCP, the honeycomb films change from extremely irregular to highly ordered structures, as highlighted with green borders. Further increasing the content of BCP leads to disordered structures, among which bimodal pores are observed for some samples. It is worth noting that the pure BCP cannot form ordered structure at this concentration (**Fig. S5**, SI).

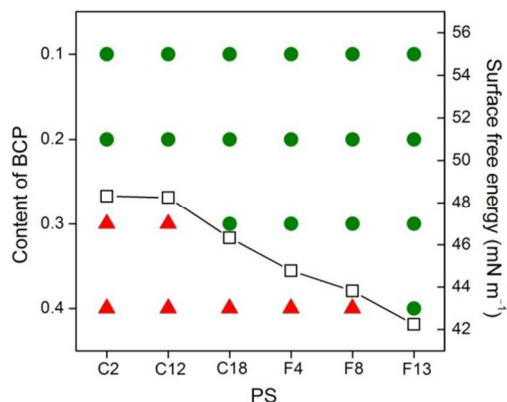


Fig. 8 Relationship between the regularity of honeycomb films and surface free energies of PS with hydrophobic end groups. The films were prepared from the mixture of PS and PS-*b*-PDMAEMA at a total concentration of 10 mg/mL. Filled green circle denotes well-ordered films while filled red triangle denotes disordered films. The surface free energies of the polymers (from C2-PS to F13-PS) are plotted using hollow black squares.

More interestingly, the evolution of the surface morphologies is dependent on not only the concentration but also the hydrophobic end groups (**Fig. 8**). Filled green circles denote ordered films whereas filled red triangles represent disordered structures. The surface free energies of the polystyrenes are also plotted in this figure. It is clear that the ordered-disordered boundary is well consistent with the trend lines of the surface free energies of the polymers. In other words, lower surface free energy of the end-functionalized polystyrenes endows them with broader film-forming window. For example, C2-PS

can be blended with a maximum of 20 wt.% BCP; however, F13-PS is able to tolerate at least 40 wt.% BCP. These results further confirmed the importance of the balance between hydrophilicity and hydrophobicity,⁶⁰⁻⁶² i.e., too hydrophobic polymers are not able to stabilize the condensed water droplets from coalescing (**Fig. S3**, SI) whereas too hydrophilic polymers lead to deteriorated and disordered structures (**Fig. S5**, SI).

The addition of BCP as well as the hydrophobic end groups also has a significant impact on the pore diameter of the honeycomb films. **Fig. 9** shows the pore diameter distribution of typical samples. It can be found that the pore diameter decreases with increasing the content of BCP. For example, F4-PS with 10 wt.% BCP produces films with a pore diameter of ~1.6 μm; it decreases to about 500 nm by increasing BCP to 30 wt.%. In addition, bimodal pores exist in some samples with a high content (40 wt.%) of the BCP. These results imply that it is easy and effective to fine-tune the pore size of honeycomb films through the polystyrenes with hydrophobic end groups using an amphiphilic block copolymer as the additive. And, the modulation can be well directed by the interfacial activities of the polymers. This proposed approach is very important to the applications of honeycomb films, such as separation membranes and templating materials.

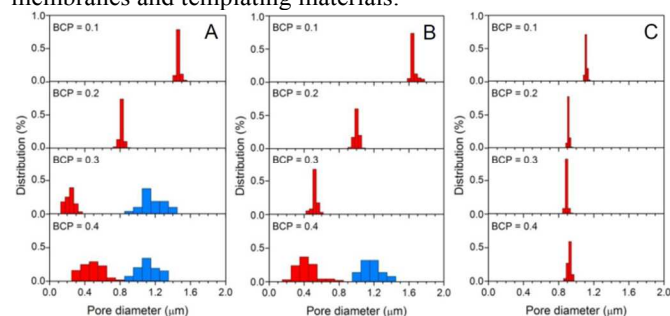


Fig. 9 Typical pore diameter distribution of films prepared from the blends of (A) C2-PS, (B) F4-PS, and (C) F13-PS with different contents of PS-*b*-PDMAEMA.

Conclusions

A series of polystyrenes with hydrophobic end groups were synthesized by the ATRP approach using six novel alkyl or fluorinated initiators. These hydrophobic initiators are effective in the ATRP of styrene, which is confirmed by the molecular weights and their distribution as well as the polymerization kinetics. It is found that the hydrophobic end groups can segregate at the film surface, and those with more fluorine atoms that have lower surface free energies show stronger interfacial activity. Honeycomb films were prepared by the breath figure method from the polystyrenes or the blends with an amphiphilic block copolymer. Polystyrenes with shorter alkyl groups and fewer fluorine atoms at the chain end are more likely to form ordered structure at high concentration (40~60 mg/mL). On the contrary, polystyrenes with long alkyl or fluorinated end groups cannot form ordered films under all the conditions we investigated. However, highly ordered structures can be obtained from the blends with only 10 wt.% amphiphilic block copolymer at much lower concentration (10 mg/mL); significantly, we found that lower surface free energy of the end-functionalized polystyrenes (more hydrophobic) endows them with broader film-forming window. It is easy and effective to fine-tune the pore size of honeycomb films through the polystyrenes with hydrophobic end groups using an amphiphilic block copolymer as the additive.

Acknowledgements

This work is supported by the National Natural Science Foundation of China (21374100 and 51173161), the Fundamental Research Funds for the Central Universities (2014QNA4037), and the State Key Laboratory of Materials-Oriented Chemical Engineering (KL13-11).

Notes and references

^a MOE Key Laboratory of Macromolecular Synthesis and Functionalization, Department of Polymer Science and Engineering, Zhejiang University, Hangzhou 310027, China. E-mail: lswan@zju.edu.cn. Phone: +86-571-87953763.

^b State Key Laboratory of Materials-Oriented Chemical Engineering, Nanjing University of Technology, Nanjing 210009, China
Electronic Supplementary Information (ESI) available: [GPC traces, XPS spectra, SEM images of honeycomb films prepared from polystyrenes with different molecular weights and at different solvents, and SEM images of PS-*b*-PDMAEMA]. See DOI: 10.1039/c000000x/

- V. Coessens, T. Pintauer and K. Matyjaszewski, *Prog. Polym. Sci.* 2001, **26**, 337-377.
- H. Willcock and R. K. O'Reilly, *Polym. Chem.* 2010, **1**, 149-157.
- C. J. Hawker, A. W. Bosman and E. Harth, *Chem. Rev.* 2001, **101**, 3661-3688.
- S. Hilf and A. F. M. Kilbinger, *Nat. Chem.* 2009, **1**, 537-546.
- A. Hirao and M. Hayashi, *Acta Polym.* 1999, **50**, 219-231.
- Y. Kim, S. Cook, J. Kirkpatrick, J. Nelson, J. R. Durrant, D. D. C. Bradley, M. Giles, M. Heeney, R. Hamilton and I. McCulloch, *J. Phys. Chem. C* 2007, **111**, 8137-8141.
- J. S. Kim, Y. Lee, J. H. Lee, J. H. Park, J. K. Kim and K. Cho, *Adv. Mater.* 2010, **22**, 1355-1360.
- C. Shim, M. Kim, S. G. Ihn, Y. S. Choi, Y. Kim and K. Cho, *Chem. Commun.* 2012, **48**, 7206-7208.
- K. L. Heredia, G. N. Grover, L. Tao and H. D. Maynard, *Macromolecules* 2009, **42**, 2360-2367.
- J. T. Xu, C. Boyer, V. Bulmus and T. P. Davis, *Polym. Sci. Part A-Polym. Chem.* 2009, **47**, 4302-4313.
- P. Kujawa, F. Segui, S. Shaban, C. Diab, Y. Okada, F. Tanaka and F. M. Winnik, *Macromolecules* 2006, **39**, 341-348.
- Y. Inoue, P. Kuad, Y. Okumura, Y. Takashima, H. Yamaguchi and A. Harada, *J. Am. Chem. Soc.* 2007, **129**, 6396-6397.
- F. D. Jochum, L. zur Borg, P. J. Roth and P. Theato, *Macromolecules* 2009, **42**, 7854-7862.
- L. Yu, H. Zhang and J. D. Ding, *Angew. Chem. Int. Ed.* 2006, **45**, 2232-2235.
- Z. Ma, Y. Y. Wang, P. Wang, W. Huang, Y. B. Li, S. B. Lei, Y. L. Yang, X. L. Fan and C. Wang, *ACS Nano* 2007, **1**, 160-167.
- L. A. Connal, R. Vestberg, C. J. Hawker and G. G. Qiao, *Adv. Funct. Mater.* 2008, **18**, 3706-3714.
- Y. Xia, N. A. D. Burke and H. D. H. Stover, *Macromolecules* 2006, **39**, 2275-2283.
- G. Widawski, M. Rawiso and B. Francois, *Nature* 1994, **369**, 387-389.
- M. Srinivasarao, D. Collings, A. Philips and S. Patel, *Science* 2001, **292**, 79-83.
- L. Song, R. K. Bly, J. N. Wilson, S. Bakbak, J. O. Park, M. Srinivasarao and U. H. F. Bunz, *Adv. Mater.* 2004, **16**, 115-118.
- J. C. Hsu, K. Sugiyama, Y. C. Chiu, A. Hirao and W. C. Chen, *Macromolecules* 2010, **43**, 7151-7158.
- J. Wang, H. X. Shen, C. F. Wang and S. Chen, *J. Mater. Chem.* 2012, **22**, 4089-4096.
- P. C. Chen, L. S. Wan, B. B. Ke and Z. K. Xu, *Langmuir* 2011, **27**, 12597-12605.
- M. H. Lu and Y. Zhang, *Adv. Mater.* 2006, **18**, 3094-3098.
- X. F. Li, L. A. Zhang, Y. X. Wang, X. L. Yang, N. Zhao, X. L. Zhang and J. A. Xu, *J. Am. Chem. Soc.* 2011, **133**, 3736-3739.
- L. S. Wan, Q. L. Li, P. C. Chen and Z. K. Xu, *Chem. Commun.* 2012, **48**, 4417-4419.
- J. L. Gong, L. C. Sun, Y. W. Zhong, C. Y. Ma, L. Li, S. Y. Xie and V. Svrcek, *Nanoscale* 2012, **4**, 278-283.
- N. E. Zander, J. A. Orticki, A. S. Karikari, T. E. Long and A. M. Rawlett, *Chem. Mater.* 2007, **19**, 6145-6149.
- D. Ishii, H. Yabu and M. Shimomura, *Chem. Mater.* 2009, **21**, 1799-1801.
- P. S. Brown, E. L. Talbot, T. J. Wood, C. D. Bain and J. P. S. Badyal, *Langmuir* 2012, **28**, 13712-13719.
- D. Beattie, K. H. Wong, C. Williams, L. A. Poole-Warren, T. P. Davis, C. Barner-Kowollik and M. H. Stenzel, *Biomacromolecules* 2006, **7**, 1072-1082.
- Y. Fukuhira, M. Ito, H. Kaneko, Y. Sumi, M. Tanaka, S. Yamamoto and M. Shimomura, *J. Biomed. Mater. Res. Part B-Appl. Biomater.* 2008, **86B**, 353-359.
- B. B. Ke, L. S. Wan and Z. K. Xu, *Langmuir* 2010, **26**, 8946-8952.
- L. S. Wan, J. W. Li, B. B. Ke and Z. K. Xu, *J. Am. Chem. Soc.* 2012, **134**, 95-98.
- H. L. Cong, J. L. Wang, B. Yu and J. G. Tang, *Soft Matter* 2012, **8**, 8835-8839.
- C. Du, A. J. Zhang, H. Bai and L. Li, *ACS Macro Letters* 2013, **2**, 27-30.
- M. H. Stenzel-Rosenbaum, T. P. Davis, A. G. Fane and V. Chen, *Angew. Chem. Int. Ed.* 2001, **40**, 3428-3432.
- L. A. Connal, R. Vestberg, C. J. Hawker and G. G. Qiao, *Adv. Funct. Mater.* 2008, **18**, 3315-3322.
- A. Bolognesi, C. Mercogliano, S. Yunus, M. Civardi, D. Comoretto and A. Turturro, *Langmuir* 2005, **21**, 3480-3485.
- L. Billon, M. Manguian, V. Pellerin, M. Joubert, O. Eterradosi and H. Garay, *Macromolecules* 2009, **42**, 345-356.
- F. Galeotti, V. Calabrese, M. Cavazzini, S. Quici, C. Poleunis, S. Yunus and A. Bolognesi, *Chem. Mater.* 2010, **22**, 2764-2769.
- L. W. Zhu, Y. Ou, L. S. Wan and Xu, Z. K., *J. Phys. Chem. B* 2014, **118**, 845-854.
- B. B. Ke, L. S. Wan, P. C. Chen, L. Y. Zhang and Z. K. Xu, *Langmuir* 2010, **26**, 15982-15988.
- L. S. Wan, B. B. Ke, X. K. Li, X. L. Meng, L. Y. Zhang and Z. K. Xu, *Sci. China Series B-Chem.* 2009, **52**, 969-974.
- D. K. Owens and R. C. Wendt, *J. Appl. Polym. Sci.* 1969, **13**, 1741-1747.
- B. M. Tande, N. J. Wagner and Y. H. Kim, *Macromolecules* 2003, **36**, 4619-4623.
- S. Sinnwell and H. Ritter, *Macromol. Rapid Commun.* 2006, **27**, 1335-1340.

48. J. E. Baez, A. Marcos-Fernandez and P. Galindo-Iranzo, *J. Polym. Res.* 2011, **18**, 1137-1146.
49. L. R. Hutchings, N. M. Sarih and R. L. Thompson, *Polym. Chem.* 2011, **2**, 851-861.
50. L. R. Hutchings, A. P. Narriainen, R. L. Thompson, N. Clarke and L. Ansari, *Polym. Int.* 2008, **57**, 163-170.
51. A. P. Narriainen, L. R. Hutchings, I. Ansari, R. L. Thompson and N. Clarke, *Macromolecules* 2007, **40**, 1969-1980.
52. S. M. Kimani, S. J. Hardman, L. R. Hutchings, N. Clarke and R. L. Thompson, *Soft Matter* 2012, **8**, 3487-3496.
53. W. N. A. Bergius, L. R. Hutchings, N. M. Sarih, R. L. Thompson, M. Jeschke and R. Fisher, *Polym. Chem.* 2013, **4**, 2815-2827.
54. B. Zuo, Y. J. Liu, L. Wang, Y. M. Zhu, Y. F. Wang and X. P. Wang, *Soft Matter* 2013, **9**, 9376-9384.
55. M. H. Stenzel, C. Barner-Kowollik and T. P. Davis, *J. Polym. Sci. Part A-Polym. Chem.* 2006, **44**, 2363-2375.
56. L. S. Wan, B. B. Ke, J. Zhang and Z. K. Xu, *J. Phys. Chem. B* 2012, **116**, 40-47.
57. A. S. Karikari, S. R. Williams, C. L. Heisey, A. M. Rawlett and T. E. Long, *Langmuir* 2006, **22**, 9687-9693.
58. Y. Xu, B. K. Zhu and Y. Y. Xu, *Polymer* 2005, **46**, 713-717.
59. B. B. Ke, L. S. Wan, Y. Li, M. Y. Xu and Z. K. Xu, *Phys. Chem. Chem. Phys.* 2011, **13**, 4881-4887.
60. J. Y. Kim, M. H. Park, M. K. Joo, S. Y. Lee and B. Jeong, *Macromolecules* 2009, **42**, 3147-3151.
61. L. Yu, Z. Zhang and J. D. Ding, *Biomacromolecules* 2011, **12**, 1290-1297.
62. C. Chen, L. Chen, L. P. Cao, W. J. Shen, L. Yu and J.D. Ding, *RSC Adv.* 2014, **4**, 8789-8798.

Graphical Abstract

Polystyrene with Hydrophobic End Groups: Synthesis, Kinetics, Interfacial Activity, and Self-assemblies Templated by Breath Figures

Liang-Wei Zhu,^a Bai-Heng Wu,^a Ling-Shu Wan^{a,b,*} and Zhi-Kang Xu^a

^a MOE Key Laboratory of Macromolecular Synthesis and Functionalization, Department of Polymer Science and Engineering, Zhejiang University, Hangzhou 310027, China.

^b State Key Laboratory of Materials-Oriented Chemical Engineering, Nanjing University of Technology, Nanjing 210009, China

E-mail: lswan@zju.edu.cn. Phone: +86-571-87953763.

Polystyrenes with hydrophobic end groups are synthesized from a series of alkyl or fluorinated ATRP initiators to fine-tune the surface morphologies of honeycomb films prepared by the breath figure method.

